A coupled WRF-PV model to investigate the local thermal environmental impacts of widespread photovoltaic plants deployment

Victor. S Olawoore, C. Lei, B. Li*, Y. Shuai

School of Energy Science and Engineering, Harbin Institute of Technology, Harbin 150001, China; biaoli@hit.edu.cn

Introduction

Photovoltaic (PV) plants are a suitable, clean and abundantly available alternative power production source increasingly adopted by different countries to mitigate climate change effects. Besides the prospects of agrophotovoltaics and PV siting, the possible effects of such widespread PV installations on the local thermal environment, energy saving and land ecology changes over time is an emerging observation in related studies[1,2]. In attempts to quantify these changes, regional climate modelling has been carried out with the weather research and forecasting (WRF) model using simple radiative fluxes or rooftop PV parameterizations within the urban canopy energy balance models[3,4].

However, little is still known of their exact impact or extent. In this study, we present a PV model coupling to Noah with multi-parameterization (Noah-MP) land surface model[5] of the WRF to conduct an extensive fine-resolution investigation of the influences of PV plants on parameters such as wind profile, temperature etc. The study strongly suggests that this WRF-based model would help to advance the current knowledge in this field and provide robust answers to the existing question of PV contributions to the local climate.

.

Modelling

Here, the Noah-MP land surface model of the WRF is parameterized such that there is a PV fraction and a bare (non-PV) land fraction. As shown in Figure 1-2, the longwave, sensible heat, latent heat and ground heat fluxes were calculated for the bare and PV land fractions separately while the Shortwave were calculated over the entire grid.

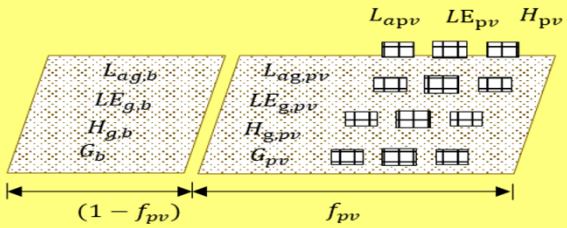

Figure 1: Schematic diagram for "semitile" subgrid scheme for the Longwave (LW), sensible heat (H), latent heat (LE) and Ground heat (G) fluxes for the bare soil and PV ground respectively. f_{pv} is PV fraction.

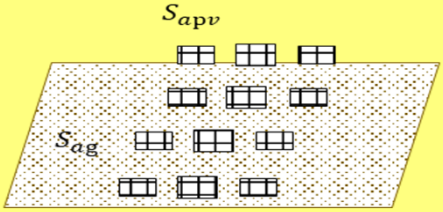

Figure 2: Schematic diagram for computation of shortwave radiation fluxes over the bare land (S_{ag}) and PV land (S_{apv}) entire grid

So that the surface energy balance equation over a grid cell is: $S_{apv} + S_{ag} = LW + LE + H + G$

$$LW = (1-f_{pv})L_{ag,b} + f_{pv}(L_{apv} + L_{ag,pv})$$
$$LE = (1-f_{pv})LE_{g,b} + f_{pv}(LE_{pv} + LE_{g,pv})$$
$$H = (1-f_{pv})H_{g,b} + f_{pv}(H_{pv} + H_{g,pv})$$
$$G = (1-f_{pv})G_b + f_{pv}G_{pv}$$

Table 1 below shows Shows the modification of the Noah-MP LSM Energy flux formation for PV land

Table 1 – Formulation of Energy fluxes over PV land surface in Noah MP

	Bare ground fraction $1-F_{pv}$	Ground within PV fraction, F_{pv}	PV fraction, F_{pv}
Longwave	$L_g = -\alpha_{gL}L_{sky}\downarrow + \varepsilon_g\sigma T_{g,b}^4$	$L_{ag,pv} = (1-\varepsilon_g)L_{sky}\downarrow + \varepsilon_g\sigma T_{g,pv}^4$	$L_{pv}^{isky} + L_{\to pv} - L_{pv}^{\uparrow} - L_{pv}^{\downarrow}$
Sensible heat	$H_{g,b} = \sigma C_p \frac{T_{g,b} - T_{air}}{r_{ah}}$	$H_{g,pv} = \sigma C_p \frac{T_{g,pv} - T_{PVCTMP}}{r_{ah,g}}$	$(h^{up} + h^{btm})(T_{pv} - T_{PVCTMP})$
Latent heat	$LE_{g,b} = \frac{\sigma C_p}{\gamma}\frac{e_{sat}(T_{g,b})h_g - e_{air}}{r_{aw} + r_{soil}}$	$LE_{g,pv} = \frac{\sigma C_p}{\gamma}\frac{e_{sat}(T_{g,pv})h_g - e_{aPVC}}{r_{aw,g} + r_{soil}}$	-
Ground heat	$G_b = \frac{2\lambda_{isno+1}}{\Delta z_{isno+1}}(T_{g,b} - T_{isno+1})$	$G_{pv} = \frac{2\lambda_{isno+1}}{\Delta z_{isno+1}}(T_{g,pv} - T_{isno+1})$	-

$r_{ah,g}$ is aerodynamic resistance below the canopy for water vapor see Niu and Yang [6]. $L_{sky}\downarrow$ is down welling longwave radiation from the sky (Wm^{-2}), T_{air} is air temperature *(K)* at reference height. e_{air} is water vapor pressure *(pa)* at reference height. e_{aPVC} is water vapor pressure of the canopy air. $e_{sat}(T_{g,pv})$, $e_{sat}(T_{g,b})$ are saturated water vapor pressure at temperature $T_{g,pv}$ and $T_{g,b}$ respectively. L_{pv}^{isky} is portion of the longwave from the sky received by the PV panel derived by the PV sky view factor[7]. Longwave radiation from adjacent PV panels $(L_{\to pv})$, Upward longwave radiation from PV $(L_{pv}^{\uparrow})$, Downward radiation from the PV bottom surface$(L_{pv}^{\downarrow})$.γ is psychrometric constant. PV temperature values at time $(t+1)$,

$$T_{PV}(t+1) = T_{PV}(t) + step \cdot \frac{\partial T_{PV}}{\partial t}$$

h^{up}, h^{btm} are turbulent convection coefficient of the upper and bottom PV parts respectively obtained from the EnergyPlus model[4,9];

T_{PVCTMP} temperature of the canopy air is derived from

$$H_{g,PV} + H_{PV} = \rho C_p \frac{T_{ac} - T_{air}}{r_{ah}}$$

$$T_{PVCTMP} = \frac{\rho C_p\left[\frac{T_{g,PV}}{r_{ah,g}} + \frac{T_{air}}{r_{ah}}\right] + [H^{up} + H^{bttm}]T_{PV}}{\rho C_p\left[\frac{1}{r_{ah,g}} + \frac{1}{r_{ah}}\right] + [H^{up} + H^{bttm}]}$$

However, in this work, since we assumed the absence of vegetation within the canopy, r_{ah} is aerodynamic resistance for heat is used instead.

Conclusions

The present work is focused mainly on the presence of PV panels on the bare land. Inclusion of vegetation growth under the PV panel is considered in the next version. With this model, we are certain that we could provide a new study field for the study of PV canopy effects as shown in figure 3 below

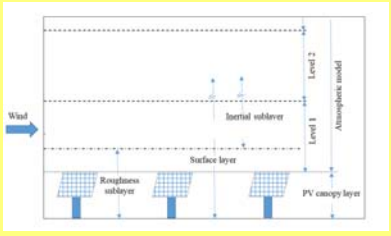

Figure 3: Schematic diagram for proposed PV canopy.

References

[1] R. Chang, Y. Yan, Y. Luo, C. Xiao, C. Wu, J. Jiang, W. Shi, A coupled WRF-PV mesoscale model simulating the near-surface climate of utility-scale photovoltaic plants, Sol. Energy. 245 (2022) 278–289. https://doi.org/10.1016/J.SOLENER.2022.09.023.

[2] S. Yue, M. Guo, P. Zou, W. Wu, X. Zhou, Effects of photovoltaic panels on soil temperature and moisture in desert areas, Environ. Sci. Pollut. Res. 28 (2021) 17506–17518. https://doi.org/10.1007/s11356-020-11742-8.

[3] H. Tan, V.R. Kotamarthi, J. Wang, Y. Qian, T. Chakraborty, Impact of Different Roofing Mitigation Strategies on Near-Surface Temperature and Energy Consumption Over the Chicago Metropolitan Area During a Heatwave Event, SSRN Electron. J. (2022) 160508. https://doi.org/10.2139/ssrn.4216263.

[4] A. Zonato, A. Martilli, E. Gutierrez, F. Chen, C. He, M. Barlage, D. Zardi, L. Giovannini, Exploring the Effects of Rooftop Mitigation Strategies on Urban Temperatures and Energy Consumption, J. Geophys. Res. Atmos. 126 (2021). https://doi.org/10.1029/2021JD035002.

[5] G.Y. Niu, Z.L. Yang, K.E. Mitchell, F. Chen, M.B. Ek, M. Barlage, A. Kumar, K. Manning, D. Niyogi, E. Rosero, M. Tewari, Y. Xia, The community Noah land surface model with multiparameterization options (Noah-MP): 1. Model description and evaluation with local-scale measurements, J. Geophys. Res. Atmos. 116 (2011) 12109. https://doi.org/10.1029/2010JD015139.

[6] G.Y. Niu, Z.L. Yang, Effects of vegetation canopy processes on snow surface energy and mass balances, J. Geophys. Res. Atmos. 109 (2004) 1–15. https://doi.org/10.1029/2004JD004884.

[7] J. Heusinger, A.M. Broadbent, D.J. Sailor, M. Georgescu, Introduction, evaluation and application of an energy balance model for photovoltaic modules, Sol. Energy. 195 (2020) 382–395. https://doi.org/10.1016/j.solener.2019.11.041.

[8] A.D. Jones, C.P. Underwood, A thermal model for photovoltaic systems, Sol. Energy. 70 (2001) 349–359. https://doi.org/10.1016/S0038-092X(00)00149-3.

[9] U.D. of Energy, US Department of Energy, EnergyPlus™ Version 22.1.0 Documentation: Engineering Reference, (2022) 94–104. https://energyplus.net/assets/nrel_custom/pdfs/pdfs_v22.1.0/EngineeringReference.pdf.